

UC San Diego

UC San Diego Previously Published Works

Title

Epigallocatechin gallate has pleiotropic effects on transmembrane signaling by altering the embedding of transmembrane domains

Permalink

<https://escholarship.org/uc/item/1mp5h5bg>

Journal

Journal of Biological Chemistry, 292(24)

ISSN

0021-9258

Authors

Ye, Feng
Yang, Chansik
Kim, Jiyoon
et al.

Publication Date

2017-06-01

DOI

10.1074/jbc.c117.787309

Peer reviewed



Epigallocatechin gallate has pleiotropic effects on transmembrane signaling by altering the embedding of transmembrane domains

Received for publication, March 22, 2017, and in revised form, May 1, 2017. Published, Papers in Press, May 9, 2017, DOI 10.1074/jbc.C117.787309

Feng Ye^{‡1}, Chansik Yang^{§¶1}, Jiyeon Kim[§], Christopher J. MacNevin^{||}, Klaus M. Hahn^{||}, Dongeun Park^{¶1}, Mark H. Ginsberg^{‡2}, and Chungho Kim^{§3}

From the [‡]Department of Medicine, University of California San Diego School of Medicine, La Jolla, California 92093, the [§]Department of Life Sciences, Korea University, Seoul 136-701, Republic of Korea, the [¶]School of Biological Sciences, Seoul National University, Seoul 151-747, Republic of Korea, and the ^{||}Department of Pharmacology and Lineberger Cancer Center, University of North Carolina at Chapel Hill, Chapel Hill, North Carolina 27599

Edited by George M. Carman

Epigallocatechin gallate (EGCG) is the principal bioactive ingredient in green tea and has been reported to have many health benefits. EGCG influences multiple signal transduction pathways related to human diseases, including redox, inflammation, cell cycle, and cell adhesion pathways. However, the molecular mechanisms of these varying effects are unclear, limiting further development and utilization of EGCG as a pharmaceutical compound. Here, we examined the effect of EGCG on two representative transmembrane signaling receptors, integrin α IIB β 3 and epidermal growth factor receptor (EGFR). We report that EGCG inhibits talin-induced integrin α IIB β 3 activation, but it activates α IIB β 3 in the absence of talin both in a purified system and in cells. This apparent paradox was explained by the fact that the activation state of α IIB β 3 is tightly regulated by the topology of β 3 transmembrane domain (TMD); increases or decreases in TMD embedding can activate integrins. Talin increases the embedding of integrin β 3 TMD, resulting in integrin activation, whereas we observed here that EGCG decreases the embedding, thus opposing talin-induced integrin activation. In the absence of talin, EGCG decreases the TMD embedding, which can also disrupt the integrin α - β TMD interaction, leading to integrin activation. EGCG exhibited similar paradoxical behavior in EGFR signaling. EGCG alters the topology of EGFR TMD and activates the receptor in the absence of EGF, but inhibits EGF-induced EGFR activation. Thus, this widely ingested polyphenol exhibits pleiotropic effects on transmembrane signaling by modifying the topology of TMDs.

Green tea has been one of the most popular drinks for thousands of years, both as a beverage and as an herbal medicine. Indeed, green tea has many clinically reported health benefits, including the prevention of cardiovascular diseases (1, 2) and cancer (3). Studies on the beneficial effects of green tea using cellular or animal models have recently converged on EGCG,⁴ the most abundant polyphenol considered as a health-promoting phytonutrient in green tea, and have found EGCG to influence multiple signal transduction pathways related to antioxidant, inflammation, cell cycle, and cell adhesion (4). However, the molecular mechanism underlying those effects has remained elusive. Although EGCG has been suggested to have a number of molecular targets (5), only DNA methyltransferase (6) and the 67-kDa laminin receptor (7) have been demonstrated to directly respond to EGCG in an *in vitro* system. On the other hand, recent nuclear magnetic resonance spectroscopy studies clearly showed that EGCG can interact with model lipid membranes (8, 9), which implies that biological membrane can be a molecular target of EGCG. Furthermore, the EGCG-lipid interaction can cause a deformation of the lipid bilayer, *e.g.* by inducing an expansion of the lipid bilayer (10) and/or altering the thickness of the membrane (11). Because membrane-receptor interactions are important in maintaining the proper TMD topology, structures, and hence function of the transmembrane receptors (12, 13), chemical and physical alteration in biological membrane may cause changes in activities of those proteins (14). However, whether such lipid-EGCG interaction contributes to cell signaling pathways and how it could account for the broad effects of EGCG on many cell signaling pathways are yet to be elucidated.

We hypothesized that EGCG exerts its effect on transmembrane receptor signaling by interacting with a lipid bilayer and thereby changing the TMD topology and signaling of a broad spectrum of transmembrane proteins. We tested this hypothesis using integrin α IIB β 3 and EGFR, two prototypical signaling receptors. Integrin α IIB β 3 is a het-

This work was supported by the Basic Science Research Program through the National Research Foundation of Korea (Grant NRF-2016R1A2B4009755) (to C.K.), by a grant from the Korea Health Technology R&D Project through the Korea Health Industry Development Institute (Grant H114C0209) (to C.K.), and by National Institutes of Health Grants CA-142833 and P41-EB002025 (to K.M.H.) and HL 078784 and HL 117807 (to M.H.G.). The authors declare that they have no conflicts of interest with the contents of this article. The content is solely the responsibility of the authors and does not necessarily represent the official views of the National Institutes of Health.

This article contains supplemental Fig. 1.

¹ Both authors contributed equally to this work.

² To whom correspondence may be addressed. Tel.: 858-822-6432; E-mail: mhginsberg@ucsd.edu.

³ To whom correspondence may be addressed. Tel.: 82-2-3290-3402; Fax: 82-2-3290-4144; E-mail: chungho@korea.ac.kr.

⁴ The abbreviations used are: EGCG, epigallocatechin gallate; EGFR, epidermal growth factor receptor; TMD, transmembrane domain; THD, talin head domain; DMPC, 1,2-dimyristoyl-*sn*-glycero-3-phosphocholine; DMPG, 1,2-dimyristoyl-*sn*-glycero-3-phospho-(1'-*rac*-glycerol); KSI, keto-steroid isomerase; MFI, mean fluorescence intensity.

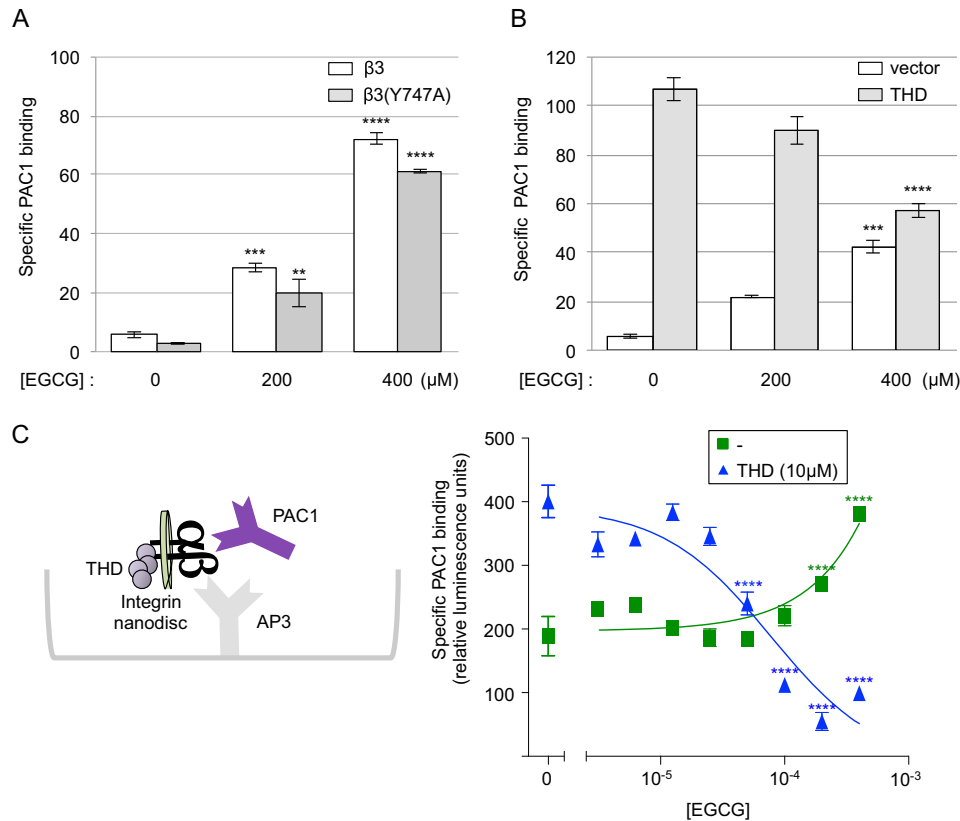


Figure 1. EGCG both activates and inhibits activation of integrin $\alpha\text{IIb}\beta 3$ in cells and a reconstituted system. *A*, CHO cells stably expressing integrin $\alpha\text{IIb}\beta 3$ were transfected with wild-type or talin binding-deficient mutant (Y747A) integrin $\beta 3$. EGCG-treated cells with comparable $\alpha\text{IIb}\beta 3$ expression (high D57 staining) were gated, and the degree of integrin activation of these gated cells was measured by PAC1, an activation-specific integrin $\alpha\text{IIb}\beta 3$ antibody. Specific PAC1 binding was calculated as $\text{MFI} - \text{MFI}_0$, where MFI is the mean fluorescence intensity of bound PAC1 and MFI_0 is that in the presence of 10 mM EDTA or 20 μM eptifibatide, both of which inhibit integrin $\alpha\text{IIb}\beta 3$ -ligand binding. *B*, CHO cells stably expressing $\alpha\text{IIb}\beta 3$ were transfected with empty vector or THD together with tdTomato cDNA as a transfection marker. Specific PAC1 binding of tdTomato-positive cells treated with different concentrations of EGCG was calculated and shown as described in *A*. *C*, the configuration of the integrin nanodisc activation assay is shown. Integrin nanodiscs were captured onto an ELISA plate coated with anti- $\beta 3$ antibody (AP3). Specific PAC1 binding was calculated as $L - L_0$, where L is PAC1 binding to the captured integrin nanodisc measured by chemiluminescence and L_0 is that in the presence of eptifibatide. The effects of EGCG on specific PAC1 binding were measured in the absence (green line) or presence of purified THD (10 μM) (blue line). Throughout the panels, error bars represent standard errors ($n = 3$), and analysis of variance multiple comparison using the Bonferroni's test was performed to test for significant differences between EGCG-treated and non-treated samples. **, $p < 0.01$; ***, $p < 0.001$; ****, $p < 0.0001$.

erodimeric transmembrane adhesion receptor that has a low affinity for its ligands in the resting state ("inactive") and a high affinity in the stimulated state ("active" or "activated"). The affinity of integrin $\alpha\text{IIb}\beta 3$ is regulated by TMD interaction of its α and β subunits (15), which depends on the precise tilt angle of the $\beta 3$ TMD determined by the lipid-protein interaction (16, 17). Indeed, the physiological integrin-activating protein, talin (18), activates the integrin by altering the tilt angle of integrin $\beta 3$ TMD (19, 20). The other model transmembrane receptor, EGFR, normally exists in an inactive monomeric state and is activated upon ligand-induced homodimerization, in which the topology of its TMD may play a role (21, 22). Here, we investigate the effect of EGCG on these two prototypical transmembrane signaling receptors and propose that EGCG can alter the membrane embedding of their TMDs, which in turn modulates transmembrane signaling by these receptors.

Results and discussion

Pleiotropic effect of EGCG on activation of integrin $\alpha\text{IIb}\beta 3$

Although EGCG is reported to have anti-thrombotic effects (23), the addition of EGCG to platelets, the main cellular medi-

ators of arterial thrombosis, causes complex responses. For example, EGCG inhibited aggregation of thrombin-stimulated platelets, but, paradoxically, caused aggregation of unstimulated platelets at the same dose (24). To better understand the physiological role of this widely consumed polyphenol, we first tested the effect of EGCG on activation of recombinant integrin $\alpha\text{IIb}\beta 3$ in CHO cells where the integrin is normally in a low affinity state; with the addition of increasing concentrations of EGCG, there was a progressive increase in activation as measured by binding of PAC1, a ligand-mimetic, activation-specific integrin $\alpha\text{IIb}\beta 3$ antibody (25) (Fig. 1A, white bars). The EGCG-induced increase in PAC1 binding was reduced by washing out EGCG (supplemental Fig. 1), showing that the effect is reversible and does not require the known oxidation-dependent reactivity toward primary amines (26). Physiological activation of this integrin requires binding of talin to the cytoplasmic domain of the $\beta 3$ subunit (27). To ask whether EGCG induces physiological activation, we utilized a mutant $\alpha\text{IIb}\beta 3(Y747A)$ that does not bind talin (28). This mutant showed similar activation by EGCG (Fig. 1A, gray bars). Thus, EGCG-induced integrin activation is not dependent on the known intracellular signaling pathway.

To directly test the effects of EGCG on talin-induced integrin activation, we introduced talin head domain (THD), the integrin-activating talin fragment (18), into CHO cells expressing integrin α IIB β 3 (CHO/ α IIB β 3), and then examined the effects of EGCG on the talin-induced activation. EGCG blocked THD-induced α IIB β 3 activation in a dose-dependent manner, whereas EGCG alone induced integrin activation (Fig. 1B).

Because of the complexity of cellular components that might mediate these paradoxical effects of EGCG, we utilized an *in vitro* reconstitution system in which purified integrin α IIB β 3 was embedded in nanodiscs, islands of 10-nm lipid bilayer encircled by membrane scaffold protein (29). In the reconstituted system, the addition of purified THD can activate the integrin (30). The integrin nanodiscs were first captured to the surface of assay plate coated with anti-integrin β 3 extracellular antibody (AP3), and the degree of integrin activation was measured by PAC1 binding to the immobilized integrin nanodiscs (Fig. 1C). EGCG activated the integrin nanodiscs in a dose-dependent manner (Fig. 1C, green line), as it did in cells. The addition of purified THD increases PAC1 binding in the system as shown previously (30), and the THD-induced increase was inhibited by the addition of an increasing amount of EGCG (Fig. 1C, blue line), showing a similar paradoxical effect of EGCG in the purified system as in cells (Fig. 1B).

To examine the effect of EGCG on activated integrins in cells, we utilized α IIB β 3(D723R) mutant, which is activated in a talin-dependent manner in CHO cells (28). The D723R mutation disrupts the electrostatic interaction between α IIB(R995) and β 3(D723), weakening the integrin α IIB- β 3 TMD interaction and thus favoring the activated state (31). The activating effect of the D723R mutant is dependent upon integrin-talin interactions, as its activation is abolished by disrupting integrin binding to endogenous talin, *e.g.* by the β 3(Y747A) mutation (28). When we added EGCG to the cells expressing α IIB β 3(D723R), in sharp contrast to the activating effect observed with the wild-type integrin, we observed that EGCG induced an initial suppression of activation that peaked at 200 μ M EGCG (Fig. 2A). At higher concentrations, however, EGCG induced activation, exhibiting a distinct biphasic effect (Fig. 2A). Next, we tested another activating mutant, α IIB β 3(L712R), in which TMD is predicted to shorten from 29 to 19 amino acids due to the polar residue in the middle of TMD (32). The activating effect of the α IIB β 3(L712R) mutant is talin-independent, as its activation is not affected by the loss of the talin-integrin interactions (28, 33). In contrast to α IIB β 3(D723R), EGCG had no significant effect on the L712R mutant (Fig. 2, B and C).

Opposing changes of integrin β 3 TMD topology by EGCG and talin

To find an explanation for these paradoxical effects, we noted the insensitivity of α IIB β 3(L712R) mutant to EGCG. This mutant activates integrin by shortening the β 3 TMD (32), whereas talin does it by increasing the lipid embedding of the β 3 TMD (19); both of these changes can alter the β 3 TMD tilt angle, thereby disrupting the α IIB- β 3 TMD interaction and leading to integrin activation (17). In addition, several studies demonstrated that EGCG can interact with phospholipids and can even decrease the thickness of a lipid bilayer (9–11), which

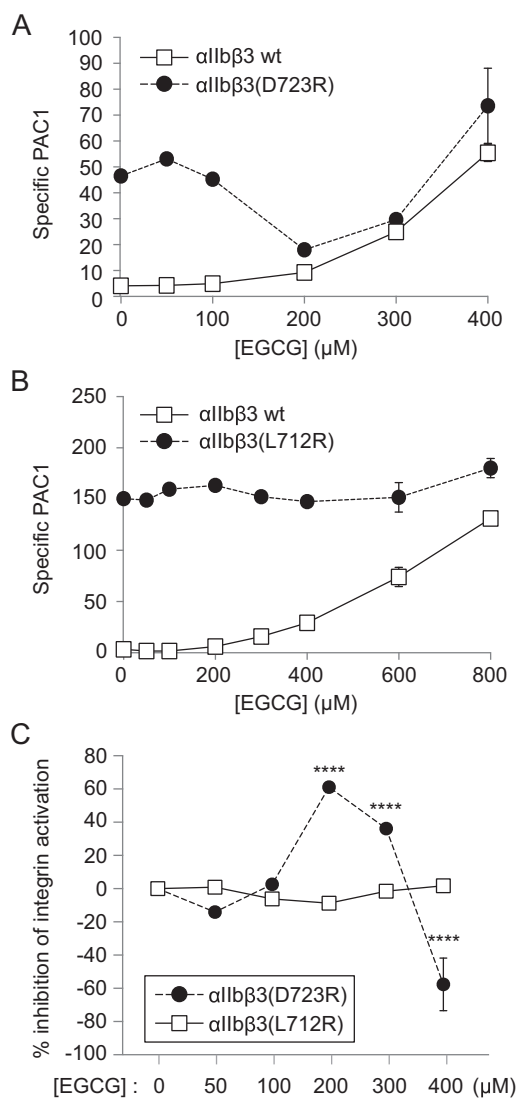


Figure 2. EGCG has distinct effects on talin-dependent and talin-independent α IIB β 3 activation. A and B, CHO cells were transfected with integrin α IIB and activating β 3 mutants, β 3(D723R) (talin-dependent) or β 3(L712R) (talin-independent), and specific PAC1 binding was measured as described in Fig. 1A. C, the percentage of inhibition of integrin activation was calculated as $100 \times (P_0 - P)/P_0$, where P_0 is the specific PAC1 binding in the absence of EGCG and P is that in the presence of EGCG. Note that EGCG initially inhibits and then increases activation of the talin-dependent α IIB β 3(D723R) mutant, whereas it does not inhibit the talin-independent α IIB β 3(L712R) mutant. Error bars represent standard errors ($n = 3$). ****, $p < 0.0001$.

may alter the lipid embedding of TMDs. To test this idea, we investigated whether EGCG can change the embedding of integrin TMD by adapting a β 3 TMD embedding assay (19). As EGCG had considerable spectral overlap with bimane, the fluorophore used in the previous study, we used another environment-sensitive fluorophore, mero60, whose fluorescence increases in a more hydrophobic environment and does not overlap with that of EGCG (34). We conjugated the dye to either the N-terminal end (β 3(L694C)) or the C-terminal end (β 3(I721C)) of β 3 TMD and reconstituted the β 3 TMD-cytoplasmic tail peptides into phospholipid nanodiscs (Fig. 3A). EGCG decreased the fluorescence of mero60 at either the N-terminal end or the C-terminal end of β 3 TMD (Fig. 3, B and C), indicating that EGCG causes both the N-terminal and the C-terminal ends of β 3 TMD to become less

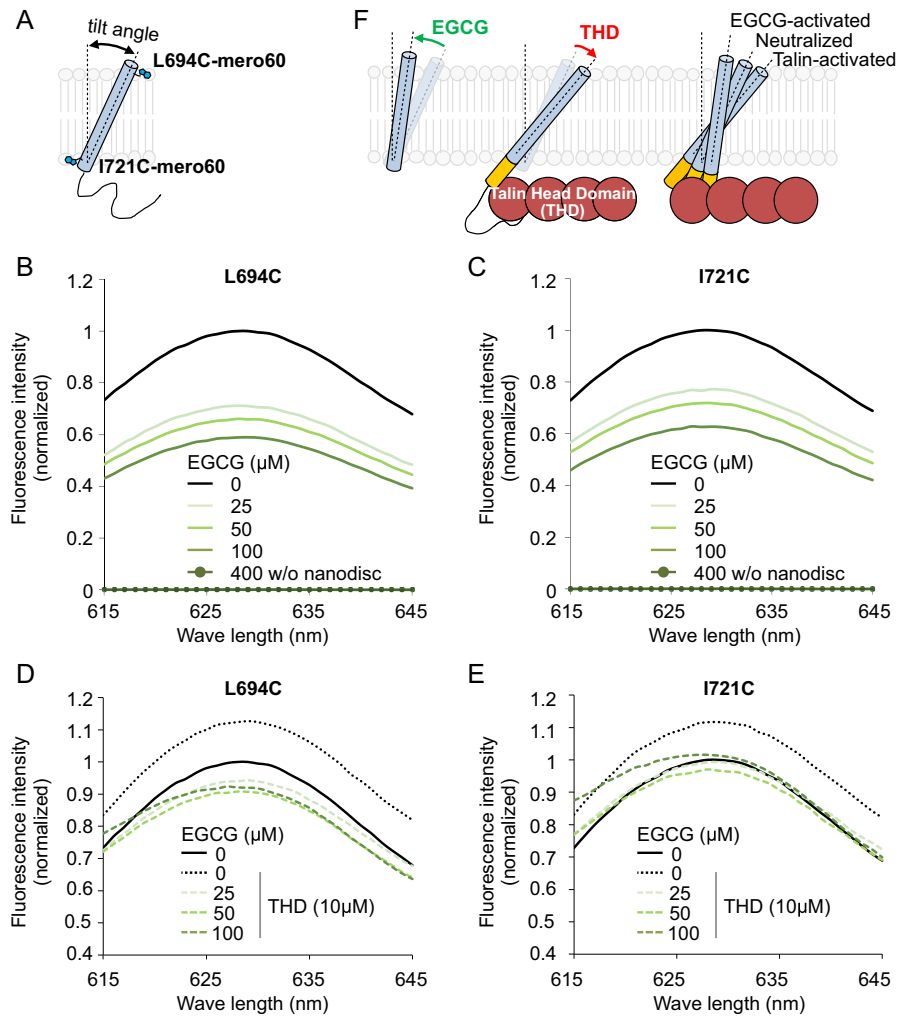


Figure 3. EGCG induces $\beta 3$ TMD topological changes in the opposite direction to talin. *A*, the environment-sensitive dye, mero60, was conjugated to $\beta 3$ TMD-tail peptide through the cysteine mutation at Leu⁶⁹⁴ residue to probe the embedding change of $\beta 3$ TMD at the outer membrane leaflet or at Ile⁷²¹ residue at the inner membrane leaflet. The mero60-labeled $\beta 3$ TMD-tail peptides were then incorporated into phospholipid nanodiscs. *B*, EGCG decreases the fluorescence intensity of L694C-mero60 nanodiscs. EGCG is not fluorescent at the wavelength range measured in the analysis. Fluorescence intensities were normalized to the maximum fluorescence intensity in the L694C-mero60 nanodiscs without EGCG. *C*, the fluorescence of I721C-mero60 nanodiscs was analyzed as in *B*. *D*, L694C-mero60 nanodiscs were incubated with 10 μM THD with or without varying concentration of EGCG. EGCG reverses the increase of mero60 fluorescence intensity induced by THD. *E*, the effect of EGCG on I721C-mero60 nanodiscs was analyzed as in *D*. *F*, proposed model of EGCG's action. Because the association of integrin αIIb and $\beta 3$ TMD depends on the precise tilt angle of $\beta 3$ TMD, either increased or decreased embedding of the $\beta 3$ TMD can disrupt the α - β TMD association and activate the integrin. Talin binding to integrin $\beta 3$ tail increases the TMD tilt angle, thereby activating integrin. EGCG interacts with the phospholipid bilayer and reduces the integrin TMD tilting angle. When both effects are present, EGCG first neutralizes the effect of talin, but continued reduction in the tilt angle by EGCG activates the integrin.

embedded. The decrease in fluorescence is a specific result from altered membrane embedding of $\beta 3$ TMD, as the EGCG-induced reduction in fluorescence disappeared after the addition of 2% SDS to disassemble the nanodisc (not shown). These data strongly suggest that EGCG reduces the embedding of the $\beta 3$ TMD, although other mechanisms, *e.g.* EGCG-induced local unraveling of the helix, cannot be ruled out. Because the optimal association of integrin αIIb and $\beta 3$ TMD depends on the precise topology of $\beta 3$ TMD (17), our data suggest that EGCG alters the $\beta 3$ TMD topology, thereby destabilizing the α - β TMD association and inducing integrin activation.

Consistent with our previous report (19) that THD increases the embedding of the $\beta 3$ TMD domain, THD increased the fluorescence intensities of mero60 conjugated to $\beta 3$ (L694C) or $\beta 3$ (I721C) (Fig. 3, *D* and *E*, *black dotted lines*). The increased fluorescence reflects an altered topology of the $\beta 3$ TMD (19),

which can also disrupt the association of integrin α and β TMDs. Intriguingly, EGCG reversed the THD-induced increase in the fluorescence of mero60 in both $\beta 3$ (L694C) and $\beta 3$ (I721C) (Fig. 3, *D* and *E*, *green dotted lines*), indicating that EGCG alters the topology of the $\beta 3$ TMD in a manner that opposes the effect of THD (Fig. 3*F*). We propose that the EGCG-induced change of the $\beta 3$ TMD topology opposes that induced by talin. Thus, it can offset the talin-induced changes in TMD topology and integrin activation. The embedding assay using integrin $\beta 3$ TMD appears more sensitive to EGCG than the integrin activation assay. In the embedding assay, concentrations of EGCG from 25 to 100 μM caused large fluorescence changes both in the absence of talin (Fig. 3, *B* and *C*) and in the presence of talin (Fig. 3, *D* and *E*), whereas higher concentrations of EGCG were required to affect the integrin activation assay (Fig. 1*C*). This may be due to the additional stabilizing

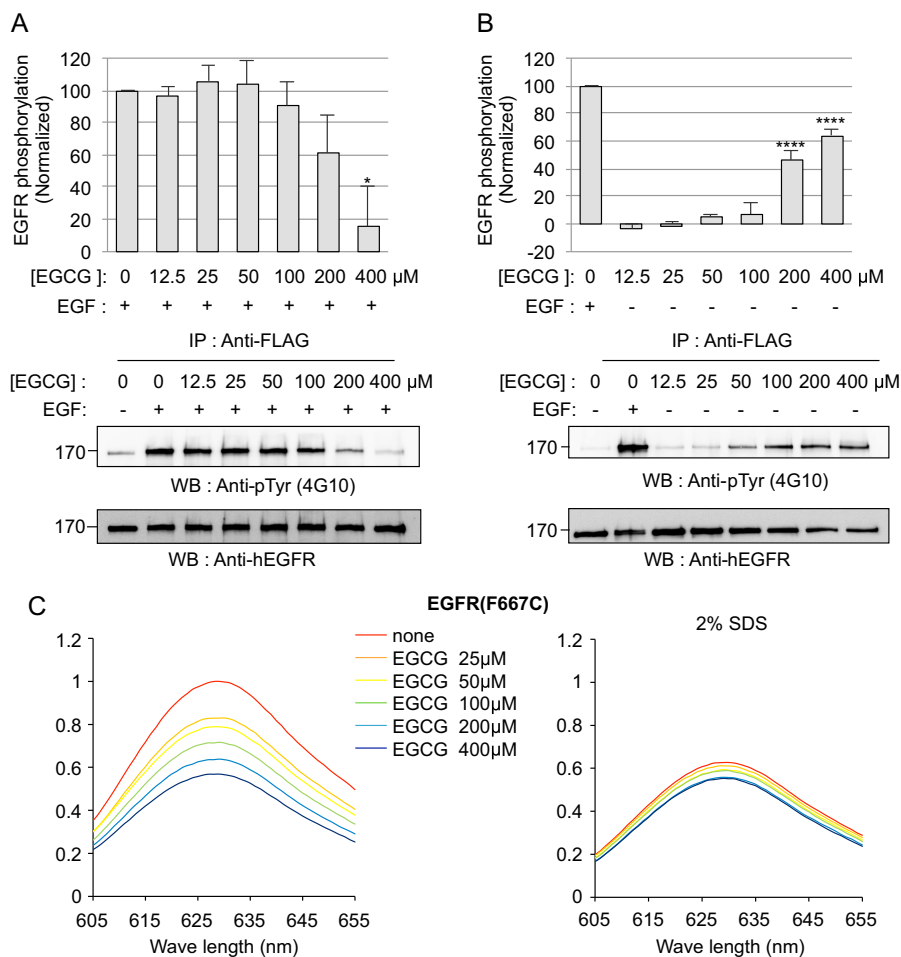


Figure 4. EGCG has a dual effect on EGFR signaling. *A*, HEK293 cells expressing FLAG-tagged human EGFR (HEK/EGFR) were serum-starved overnight and pretreated with different concentrations of EGCG. 30 min after EGCG treatment, cells were stimulated with 50 ng/ml EGF for an additional 30 min. EGFR was immunoprecipitated (IP) and analyzed by Western blotting (WB) with anti-phosphotyrosine antibody (4G10) and anti-EGFR antibody. The degree of phosphotyrosine signal per precipitated EGFR band intensities was normalized to unstimulated control (0%) and EGF-treated control (100%), and shown as a bar graph for each sample. Error bars represent standard errors ($n = 3$). Representative Western blots are shown below. *B*, phosphorylation of unstimulated EGFR in the presence of different concentrations of EGCG was analyzed as in *A*. EGCG induced EGFR phosphorylation in a dose-dependent manner. Error bars represent standard errors ($n = 3$). For panels *A* and *B*, one-way analysis of variance multiple comparison using the Bonferroni's test was performed to test for significant differences between EGCG-treated and non-treated samples. *, $p < 0.05$; ****, $p < 0.0001$. *C*, effects of EGCG on lipid embedding of EGFR TMD. *Left*, purified EGFR TMD peptide (EGFR(F667C)) labeled with mero60 was reconstituted into nanodiscs, and the effect of EGCG on the embedding of EGFR TMD was analyzed as in Fig. 3*B*. *Right*, EGCG had little effect on mero60 fluorescence when EGFR TMD nanodiscs were solubilized with 2% SDS.

effect of the presence of the extracellular domains, which are absent in the $\beta 3$ TMD embedding assays, on integrin $\alpha\beta$ association and activation.

Effects of EGCG on transmembrane signaling through a receptor tyrosine kinase

If the EGCG-induced topological change of integrin $\beta 3$ TMD is due to an EGCG-lipid interaction, we reasoned that EGCG should also have effects on other transmembrane proteins with signaling functions. To test this hypothesis, we focused on the receptor tyrosine kinases because the dimerization of their TMDs in the lipid bilayer may play a role in activation of those receptors (21, 22). Indeed, EGCG was reported to inhibit activation of receptor tyrosine kinases such as EGFR (35, 36), possibly due to effects on lipid order (36). Pretreatment of HEK293 cells stably expressing EGFR with EGCG inhibited EGF-induced EGFR phosphorylation (Fig. 4*A*). In contrast, EGCG treatment in the absence of EGF induced EGFR phosphorylation in a concentration-dependent

manner (Fig. 4*B*). Furthermore, EGCG decreased the fluorescence intensity of mero60 attached to the C-terminal region of the nanodisc-embedded EGFR TMD (Fig. 4*C*). These data suggest that a topological change of EGFR TMD induced by EGF (37) can be reversed by the action of EGCG, and that EGCG-induced topological change in the absence of EGF may favor dimerization of EGFR TMDs, leading to activation.

Our results show that EGCG can change the TMD topologies of receptors and activate those receptors. Conversely, when physiological activation involves shifts in TMD topology, then EGCG can oppose those shifts and inhibit transmembrane signaling. We propose that such a dual effect can account for the conflicting reported effects of EGCG. Recent studies showed that EGCG can bind to lipid bilayers and reside near the phosphate head groups of phospholipids, and that the interaction is further stabilized by cation- π interaction between one of the ring structures in EGCG and the quaternary amine of the phospholipid head group (8). Because the interactions between

TMDs and phospholipids can influence the topology of TMDs in a lipid bilayer by mechanisms such as snorkeling of the basic lysine side chain into the phosphate head groups of the phospholipids (16), EGCG may alter the interaction of the TMD with the phosphate head group, thus leading to changes in TMD topology. Alternatively, the rigidity of lipids induced by insertion of EGCG into hydrophobic lipid bilayer, as suggested by molecular simulation study (38), or the rigidity of lipid-inserted EGCG itself, due to its less flexible aromatic rings, might alter the tilt angle of TMDs, causing less embedding. Future studies will be required to address these hypotheses; however, our observation that EGCG has a dual effect on transmembrane signaling by modulating lipid embedding of TMDs provides an attractive mechanism to explain some of EGCG's pleiotropic effects on transmembrane signaling.

Experimental procedures

Reagents, cell lines, and plasmids

1,2-Dimyristoyl-*sn*-glycero-3-phosphocholine (DMPC) and 1,2-dimyristoyl-*sn*-glycero-3-phospho-(1'-*rac*-glycerol) (DMPG) were purchased from Avanti Polar Lipids, Inc. Membrane scaffold protein (MSP1D1) was kindly provided by Dr. Stephen Sligar (University of Illinois at Urbana-Champaign). PAC1 and D57 were described previously (16). Anti-FLAG antibody (M2) and anti-phosphotyrosine antibody (4G10) were purchased from Sigma-Aldrich and Merck Millipore, respectively. CHO/ α Ib and CHO/ α Ib β 3 cells were generated by infecting CHO cells with lentivirus encoding α Ib and/or β 3 as described previously (16). HEK/EGFR cells were kindly provided by Dr. Seung-Taek Lee (Yonsei University). The β 3 TMD-tail fused with N-terminal His₆ and ketosteroid isomerase (KSI) in the pET-31 expression vector was described previously (19). Similarly, the EGFR TMD (Pro⁶³⁷-Gln⁷⁰¹) construct containing N-terminal His₆ and KSI with cysteine mutation at Phe⁶⁶⁷ was generated by ligation of the PCR-amplified EGFR TMD region into the pET-31 expression vector.

Flow cytometry

Transfection and flow cytometry were performed with a similar procedure as described before (23). Briefly, CHO or CHO/ α Ib cells were transfected with various integrin constructs using Lipofectamine LTX and Plus reagents (Life Technologies) or Lipofectamine 2000 (Life Technologies). CHO/ α Ib β 3 cells were transfected with a total of 10 μ g of plasmids, including 1 μ g of tdTomato cDNA as a transfection marker. At 24 h after transfection, cells were detached by trypsinization and treated with EGCG for 10 min. Those cells were stained with PAC1 followed by allophycocyanin-conjugated anti-mouse IgM antibody. When integrin constructs were transfected, cells were co-stained with D57 to gate cells with similar high α Ib β 3 expression.

EGFR phosphorylation assay

Serum-starved subconfluent HEK/EGFR cells were treated with varying concentrations of EGCG for 30 min before EGF treatment (final 50 ng/ml). Cells were lysed by a lysis buffer (20 mM HEPES, pH 7.4, 150 mM NaCl, 1% Triton X-100, 10 mM EDTA, pH 7.4, supplemented with PhosSTOP (Roche Applied

Science) and protease inhibitor cocktail (Roche Applied Science)). After clarification by centrifugation at 17,000 \times *g* for 30 min, the clarified lysates were incubated at 4 °C overnight in the presence of 3 μ g of anti-FLAG antibody, and the bound proteins were precipitated with protein G-Sepharose. The bound proteins were analyzed by SDS-PAGE and subsequent Western blotting with anti-phosphotyrosine antibody and anti-EGFR antibody.

Expression and purification of TMD peptides

The preparation of integrin nanodiscs was performed essentially as described previously (19). Briefly, His₆-KSI-fused TMD proteins were expressed in *Escherichia coli* BL21(DE3) and purified using a HiTrap Chelating HP column charged with Ni²⁺. The Asp-Pro bond between KSI and TMD peptide in the purified TMD proteins was cleaved in 10% formic acid for 120 min at 80 °C (24). The resulting TMD peptide was then dialyzed against a buffer containing 50 mM Tris-HCl, pH 7.4, 500 mM NaCl, and 6 M urea, and then passed through a Ni²⁺-nitrilotriacetic acid column again to absorb the KSI, leaving the purified TMD peptide in the solution. The TMD peptide was labeled with excess mero60 (1:5 molar ratio). 0.1% Triton X-100 was added to the labeled TMD peptide, and the labeled TMD peptide was then dialyzed extensively against 0.1% Triton X-100 in Tris-buffered saline (20 mM Tris-HCl, pH 7.4, 150 mM NaCl).

Preparation of integrin nanodiscs

The preparation of integrin nanodiscs was previously described (25). Briefly, DMPC and DMPG lipids were dissolved in chloroform or chloroform/methanol mixture, mixed into a 1:1 ratio, and dried onto a glass tube with a steady flow of argon. The lipid mixture was dissolved in 100 mM cholate in TBS. To assemble nanodiscs, 360 μ l of the 1:1 lipid mixture (50 mM), 1 ml of 200 μ M MSP1D1, and the purified TMD peptides (10 μ M) or the purified integrin α Ib β 3 from human platelets (10 μ M) were mixed. The mixture was added with 2 volumes of Bio-Beads SM-2 (Bio-Rad) to initiate nanodisc assembly and incubated overnight at room temperature in the dark. The assembled nanodiscs were further purified with a size-exclusion column (HiLoad 16/60 Superdex 200) with TBS as the column buffer. When necessary, the nanodiscs were concentrated using an Amicon Ultra centrifugal filter unit with Ultracel-30 membrane (Millipore).

Fluorescence spectroscopy

200 μ l of the purified nanodiscs were mixed with 50 μ l of various concentrations of EGCG (and THD in the case of β 3 TMD nanodiscs). After 30 min of incubation at room temperature, the emission spectrum (from 605 to 655 nm) at the excitation wavelength, 593 nm, was scanned with a 1-nm interval using a FluoroMax-2 Spectrofluorometer (HORIBA Scientific). The fluorescence from unlabeled TMD peptide, talin, empty nanodiscs, or buffer was negligible. The fluorescence of the samples was re-measured after the addition of 2% SDS (final concentration).

Author contributions—F. Y., M. H. G., and C. K. designed the research. F. Y., C. Y., and J. K. performed experiments. C. J. M. and K. M. H. synthesized the fluorescent dye. F. Y., C. Y., D. P., M. H. G., and C. K. analyzed the data. F. Y., C. Y., and C. K. wrote the manuscript, which was edited by M. H. G.

Acknowledgments—We thank Se-Jong Kim, Si Hoon Park, and Dr. Hyun Kyu Song (Korea University) for technical support and helpful discussion.

References

- Kuriyama, S. (2008) The relation between green tea consumption and cardiovascular disease as evidenced by epidemiological studies. *J. Nutr.* **138**, 1548S–1553S
- Babu, P. V., and Liu, D. (2008) Green tea catechins and cardiovascular health: an update. *Curr. Med. Chem.* **15**, 1840–1850
- Shimizu, M., Adachi, S., Masuda, M., Kozawa, O., and Moriwaki, H. (2011) Cancer chemoprevention with green tea catechins by targeting receptor tyrosine kinases. *Mol. Nutr. Food Res.* **55**, 832–843
- Singh, B. N., Shankar, S., and Srivastava, R. K. (2011) Green tea catechin, epigallocatechin-3-gallate (EGCG): mechanisms, perspectives and clinical applications. *Biochem. Pharmacol.* **82**, 1807–1821
- Patra, S. K., Rizzi, F., Silva, A., Rugina, D. O., and Bettuzzi, S. (2008) Molecular targets of (–)-epigallocatechin-3-gallate (EGCG): specificity and interaction with membrane lipid rafts. *J. Physiol. Pharmacol.* **59**, Suppl. 9, 217–235
- Lee, W. J., Shim, J. Y., and Zhu, B. T. (2005) Mechanisms for the inhibition of DNA methyltransferases by tea catechins and bioflavonoids. *Mol. Pharmacol.* **68**, 1018–1030
- Tachibana, H., Koga, K., Fujimura, Y., and Yamada, K. (2004) A receptor for green tea polyphenol EGCG. *Nat. Struct. Mol. Biol.* **11**, 380–381
- Uekusa, Y., Kamihira-Ishijima, M., Sugimoto, O., Ishii, T., Kumazawa, S., Nakamura, K., Tanji, K., Naito, A., and Nakayama, T. (2011) Interaction of epicatechin gallate with phospholipid membranes as revealed by solid-state NMR spectroscopy. *Biochim. Biophys. Acta* **1808**, 1654–1660
- Scheidt, H. A., Pampel, A., Nissler, L., Gebhardt, R., and Huster, D. (2004) Investigation of the membrane localization and distribution of flavonoids by high-resolution magic angle spinning NMR spectroscopy. *Biochim. Biophys. Acta* **1663**, 97–107
- Tamba, Y., Ohba, S., Kubota, M., Yoshioka, H., Yoshioka, H., and Yamazaki, M. (2007) Single GUV method reveals interaction of tea catechin (–)-epigallocatechin gallate with lipid membranes. *Biophys. J.* **92**, 3178–3194
- Sun, Y., Hung, W. C., Chen, F. Y., Lee, C. C., and Huang, H. W. (2009) Interaction of tea catechin (–)-epigallocatechin gallate with lipid bilayers. *Biophys. J.* **96**, 1026–1035
- Lee, A. G. (2003) Lipid-protein interactions in biological membranes: a structural perspective. *Biochim. Biophys. Acta* **1612**, 1–40
- Killian, J. A., and von Heijne, G. (2000) How proteins adapt to a membrane-water interface. *Trends Biochem. Sci.* **25**, 429–434
- Escribá, P. V., González-Ros, J. M., Goñi, F. M., Kinnunen, P. K., Vigh, L., Sánchez-Magraner, L., Fernández, A. M., Busquets, X., Horváth, I., and Barceló-Coblijn, G. (2008) Membranes: a meeting point for lipids, proteins and therapies. *J. Cell Mol. Med.* **12**, 829–875
- Iwamoto, D. V., and Calderwood, D. A. (2015) Regulation of integrin-mediated adhesions. *Curr. Opin. Cell Biol.* **36**, 41–47
- Kim, C., Schmidt, T., Cho, E. G., Ye, F., Ulmer, T. S., and Ginsberg, M. H. (2011) Basic amino-acid side chains regulate transmembrane integrin signalling. *Nature* **481**, 209–213
- Lau, T. L., Kim, C., Ginsberg, M. H., and Ulmer, T. S. (2009) The structure of the integrin α IIb β 3 transmembrane complex explains integrin transmembrane signalling. *EMBO J.* **28**, 1351–1361
- Calderwood, D. A., Zent, R., Grant, R., Rees, D. J., Hynes, R. O., and Ginsberg, M. H. (1999) The Talin head domain binds to integrin β subunit cytoplasmic tails and regulates integrin activation. *J. Biol. Chem.* **274**, 28071–28074
- Kim, C., Ye, F., Hu, X., and Ginsberg, M. H. (2012) Talin activates integrins by altering the topology of the β transmembrane domain. *J. Cell Biol.* **197**, 605–611
- Kalli, A. C., Campbell, I. D., and Sansom, M. S. (2011) Multiscale simulations suggest a mechanism for integrin inside-out activation. *Proc. Natl. Acad. Sci. U.S.A.* **108**, 11890–11895
- Endres, N. F., Das, R., Smith, A. W., Arkhipov, A., Kovacs, E., Huang, Y., Pelton, J. G., Shan, Y., Shaw, D. E., Wemmer, D. E., Groves, J. T., and Kuriyan, J. (2013) Conformational coupling across the plasma membrane in activation of the EGF receptor. *Cell* **152**, 543–556
- Arkhipov, A., Shan, Y., Das, R., Endres, N. F., Eastwood, M. P., Wemmer, D. E., Kuriyan, J., and Shaw, D. E. (2013) Architecture and membrane interactions of the EGF receptor. *Cell* **152**, 557–569
- Kang, W. S., Lim, I. H., Yuk, D. Y., Chung, K. H., Park, J. B., Yoo, H. S., and Yun, Y. P. (1999) Antithrombotic activities of green tea catechins and (–)-epigallocatechin gallate. *Thromb. Res.* **96**, 229–237
- Lill, G., Voit, S., Schrör, K., and Weber, A. A. (2003) Complex effects of different green tea catechins on human platelets. *FEBS Lett.* **546**, 265–270
- Shattil, S. J., Hoxie, J. A., Cunningham, M., and Brass, L. F. (1985) Changes in the platelet membrane glycoprotein IIb/IIIa complex during platelet activation. *J. Biol. Chem.* **260**, 11107–11114
- Palhano, F. L., Lee, J., Grimster, N. P., and Kelly, J. W. (2013) Toward the molecular mechanism(s) by which EGCG treatment remodels mature amyloid fibrils. *J. Am. Chem. Soc.* **135**, 7503–7510
- Shattil, S. J., Kim, C., and Ginsberg, M. H. (2010) The final steps of integrin activation: the end game. *Nat. Rev. Mol. Cell Biol.* **11**, 288–300
- Wegener, K. L., Partridge, A. W., Han, J., Pickford, A. R., Liddington, R. C., Ginsberg, M. H., and Campbell, I. D. (2007) Structural basis of integrin activation by talin. *Cell* **128**, 171–182
- Denisov, I. G., Grinkova, Y. V., Lazarides, A. A., and Sligar, S. G. (2004) Directed self-assembly of monodisperse phospholipid bilayer Nanodiscs with controlled size. *J. Am. Chem. Soc.* **126**, 3477–3487
- Ye, F., Hu, G., Taylor, D., Ratnikov, B., Bobkov, A. A., McLean, M. A., Sligar, S. G., Taylor, K. A., and Ginsberg, M. H. (2010) Recreation of the terminal events in physiological integrin activation. *J. Cell Biol.* **188**, 157–173
- Hughes, P. E., Diaz-Gonzalez, F., Leong, L., Wu, C., McDonald, J. A., Shattil, S. J., and Ginsberg, M. H. (1996) Breaking the integrin hinge: a defined structural constraint regulates integrin signaling. *J. Biol. Chem.* **271**, 6571–6574
- Partridge, A. W., Liu, S., Kim, S., Bowie, J. U., and Ginsberg, M. H. (2005) Transmembrane domain helix packing stabilizes integrin α IIb β 3 in the low affinity state. *J. Biol. Chem.* **280**, 7294–7300
- Nieves, B., Jones, C. W., Ward, R., Ohta, Y., Reverte, C. G., and LaFlamme, S. E. (2010) The NPIY motif in the integrin β 1 tail dictates the requirement for talin-1 in outside-in signaling. *J. Cell Sci.* **123**, 1216–1226
- MacNevin, C. J., Gremyachinskiy, D., Hsu, C. W., Li, L., Rougie, M., Davis, T. T., and Hahn, K. M. (2013) Environment-sensing merocyanine dyes for live cell imaging applications. *Bioconjug. Chem.* **24**, 215–223
- Liang, Y. C., Lin-shiau, S. Y., Chen, C. F., and Lin, J. K. (1997) Suppression of extracellular signals and cell proliferation through EGF receptor binding by (–)-epigallocatechin gallate in human A431 epidermoid carcinoma cells. *J. Cell Biochem.* **67**, 55–65
- Adachi, S., Nagao, T., Ingolfsson, H. I., Maxfield, F. R., Andersen, O. S., Kopelovich, L., and Weinstein, I. B. (2007) The inhibitory effect of (–)-epigallocatechin gallate on activation of the epidermal growth factor receptor is associated with altered lipid order in HT29 colon cancer cells. *Cancer Res.* **67**, 6493–6501
- Moriki, T., Maruyama, H., and Maruyama, I. N. (2001) Activation of preformed EGF receptor dimers by ligand-induced rotation of the transmembrane domain. *J. Mol. Biol.* **311**, 1011–1026
- Sirk, T. W., Brown, E. F., Friedman, M., and Sum, A. K. (2009) Molecular binding of catechins to biomembranes: relationship to biological activity. *J. Agric. Food Chem.* **57**, 6720–6728